Time-Resolved Optical Kerr Effect Measurements in Aqueous Ionic Solutions

ARTICLE *in* THE JOURNAL OF PHYSICAL CHEMISTRY A · APRIL 1994

Impact Factor: 2.69 · DOI: 10.1021/j100082a047

Time-Resolved Optical Kerr Effect Measurements in Aqueous Ionic Solutions

I. Santa,† P. Foggi, R. Righini, and J. H. Williams*

European Laboratory for Non-Linear Spectroscopy, University of Florence, Largo E. Fermi, 2 (Arcetri), I-50125 Florence, Italy, Science, Thomas House, George IV Street, Cambridge CB2 1HH, U.K., and Department of Physics, Janus Pannonius University, Pécs, Ifjusag u.6, Hungary

Received: December 21, 1993; In Final Form: April 24, 1994®

We report the molecular dynamics of several solvated ions present in aqueous ionic solutions (HCl, HNO_3, NaCl, and $NaNO_3$) investigated by femtosecond time-resolved optical Kerr effect measurements. From the accurate fitting of decay curves, measured over 5–6 decades of intensity range, it has been possible to characterize (i) an instantaneous electronic response, (ii) a fast contribution of water, (iii) a rotational relaxation of the individual ions ($\tau_{rot} \sim 2$–3 ps), and (iv) a slow concentration–dependent decay connected to the direct ion–ion interactions. These results will be of interest to those seeking to measure electro-optic effects in aqueous solutions as these experiments give new information on the nature of the aqueous state.

Introduction

Even though the aqueous state is ubiquitous, a detailed understanding of its microscopic structure remains elusive. For example, there is a paucity of experimental data concerning the electric and magnetic properties of the solvated ions which constitute the solution. This state of affairs is largely the result of the lack of suitable techniques for the study of the electro-optic properties of solvated ions. Here we have undertaken a series of measurements of the optical Kerr effect (OKE) in various aqueous solutions. These experiments have demonstrated the suitability of this technique for such studies.

Traditionally, the static Kerr effect has been used to make measurements of the bulk electric susceptibility of a fluid. The full theory of the Kerr effect has been described previously[1,2] and has long been used as a means of obtaining molecular information[2] and, more recently, to explore the properties and dynamics of condensed phases.[3]

Application of an intense electromagnetic field to a fluid induces an anisotropy in its physical properties. The static Kerr effect is the response of a fluid to a strong uniform static electric field. The field gives rise to differences between the components of the refractive index parallel and perpendicular to the field; thus a beam of linearly polarized light propagating perpendicular to the field direction with its plane of polarization at 45° to the field becomes elliptically polarized on passage through the fluid. Physically the molecules are being oriented by the applied electric field, and the fluid is thus behaving as a uniaxial crystal, with its optic axis parallel to the field. One may perform the measurement as a function of sample temperature or of solute concentration; however, one is limited, in such a static Kerr effect experiment, to the amount of information that is available experimentally. There is only one measurable quantity, the intensity of light passing the crossed analyzer.

We may define a Kerr constant, K

$$K = (n_{\parallel} - n_{\perp})\nu/E^2 \qquad (1)$$

where $(n_{\parallel} - n_{\perp})$ is the difference between the components of the refractive index, n, for electromagnetic waves of wave number ν with electric vectors parallel and perpendicular to the field direction, the electric field, E, being uniform and normal to the optical path. In the static Kerr measurement, the permanent molecular electric dipole moment makes the largest contribution to the observed induced birefringence, provided the electric field is applied at a frequency sufficiently low as to allow the dipoles time to orient in the applied field. However, for the solutions of interest here, the static Kerr effect is a technique of limited use since ionic solutions conduct. To circumvent this problem, one could use pulsed (radio frequency) applied electric fields.[4] The other variation on the Kerr effect which allows for measurements on conducting fluids is the optical Kerr effect.[5]

In the OKE the applied electric field oscillates at optical frequencies; consequently, the dipole contribution to the measured bulk susceptibility is lost. For water, values of both Kerr constants exist in the literature; Aroney et al.[6] have measured the static Kerr constant, K^s, at 632.8 nm and 20 °C to be $2.96 \pm 0.08 \times 10^{-14}$ V^{-2} m. The optical Kerr constant of water, K^o, was first measured by Paillette[7] at 488 nm which, scaled to 632.8 nm, gives 2.48×10^{-16} V^{-2} m. The large difference between K^s and K^o arises because of the loss of the large dipolar contribution to the temperature-dependent orientation term. The permanent molecular dipole moments are, at optical frequencies, unable to follow the reversals of the applied electric field, and one is left with the contribution to the induced birefringence arising from the distortion and orientation of the molecular polarizability.

The first studies of the optical Kerr effect in aqueous ionic solutions were the measurements of Paillette.[7,8] Here, the applied oscillating electric field was that associated with the light of a pulsed ruby laser, $\lambda = 694.3$ nm. This field had a pulse width at half-maximum of between 24 and 40×10^{-9} s with a peak power of 40 MW cm^{-2}. We may then calculate the peak applied electric field as $E = \sqrt{\bar{W}/c\epsilon_0}$ giving, for $\bar{W} = 40 \times 10^6$ W cm^{-2}, $E = 1.2 \times 10^7$ V m^{-1}, a value larger than most available applied laboratory static electric fields. The associated magnetic field, which would be a source of high-frequency magnetic birefringence, is a factor c (2.998×10^8 m s^{-1}) smaller and is negligible. This pulsed laser is the source of the orienting electric field, and the degree of induced orientation is measured with a second, lower power laser, in Paillette's work an argon laser at 488.0 nm. In our present pulsed optical Kerr effect experiments, the laser pulse width is of the order of 200 fs, and the peak power of the orienting beam is 10^9 W, giving an applied oscillating electric field of the order of 10^7 V m^{-1} in a weakly focused (beam waist, of order 150 μm) beam.

The present experiments involve time-resolved OKE measurements. Here, very narrow intense pulses of light are incident upon the sample, and one measures not only a modulation of the light intensity passing the analyzer but also a temporal evolution

* To whom correspondence should be addressed at Science, Thomas House.
† Janus Pannonius University.
® Abstract published in *Advance ACS Abstracts*, July 15, 1994.

0022-3654/94/2098-7692$04.50/0

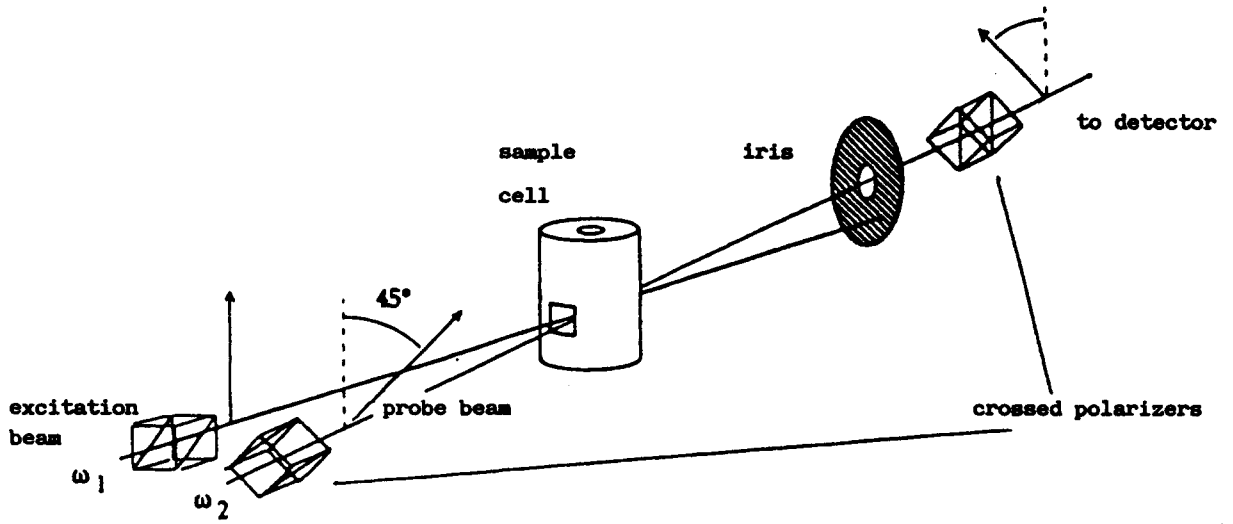

Figure 1. Schematic representation of a typical femtosecond optical Kerr effect laser system, the TROKE experimental setup at the European Laboratory for Nonlinear Spectroscopy, Florence, Italy. The two incoming laser beams are at frequencies ω_1 and ω_2; the former, the excitation beam, is the more intense and induces a birefringence in the medium which is then probed by the weaker probe beam. The polarization of the probe beam is at 45° to that of the excitation beam and is crossed with respect to the analyzer or second polarizer. The iris serves as a beam stop for the intense laser excitation beam.

of the pulse as it responds to the different degrees of freedom of the molecules or ions in the sample. For example, there is the instantaneous response of the electrons of the sample molecules followed by the slower nuclear response. The light pulses are very narrow, of the order of 100 fs, allowing us to observe directly the different frequency regimes of molecular dynamics in the condensed phase.

The works of Kenney-Wallace et al.,[9-12] Nelson et al.,[13] and McMorrow,[14,15] who all used short (<100 fs) optical pulses in their experiments, clearly showed the complex dynamics of even nonassociated pure organic liquids that the OKE can reveal in the short time domain. In brief, five contributions to the time-resolved OKE can be distinguished: (i) an instantaneous purely electronic response due to the molecular electric hyperpolarizability γ; (ii) an intermolecular librational contribution originating from the librational motion of the target molecule within the cage of solvent nearest-neighbor molecules. It decays with the lifetime of the cage, of order <200 fs. (iii) An intramolecular vibrational contribution, decaying with the dephasing time of the molecular vibrations, typically a few hundred femtoseconds; (iv) a term arising from molecular interactions, correlated to the density fluctuations and therefore to the collision-induced anisotropy of the molecular polarizability. Here the relaxation is governed by the lifetime of the local structure in the liquid, again a few hundreds of femtoseconds. (v) A rotational contribution, whose time scale can span a wide range of decay rates, from a few picoseconds to several nanoseconds, depending on the molecular size and on the viscosity of the solution.

Ultrafast solvent relaxation dynamics of ionic solutions have not been extensively investigated. Cheng and Castner[16,17] have measured the dynamics of pure water using optical-heterodyne OKE. Although this technique is capable of observing the small electronic response of water, it has only recently shown itself sensitive enough for observing the much weaker nuclear contribution to the OKE. Here, we demonstrate that we are able to observe, in aqueous solutions of simple electrolytes, the several contributing relaxation mechanisms in the 100 fs to 20 ps time scale and the 5–6 orders of magnitude change in the intensity.

The OKE is of particular advantage for the investigation of condensed phase physical phenomena. If the species of interest, whether molecule or ion, can be oriented in an applied laboratory electric field, then one may determine, by suitable polarization selection of the probing light beam, the distribution of polarizable matter in the oriented sample. That is, one may measure the mean polarizability parallel and perpendicular to the electric vector of the laser beam used to investigate the oriented sample. This difference, the induced birefringence, or retardation may be related to molecular properties. For ionic solutions, the refractive index gives the mean polarizability of a solvated ion while the induced birefringence measurement yields the fluctuations in the polarizability anisotropy of the solvated ion, which is seen to be different for solvated sodium and chloride ions compared, at a similar concentration level, with solvated nitrate ions. These birefringence measurements being made with high precision, an induced retardation of 10^{-7} rad is readily measured, which corresponds to a measured difference in the parallel and perpendicular components of the refractive indix ($n_\parallel - n_\perp$) of 9×10^{-13} at 600 nm for a 1 cm path length.

Experimental Details

A schematic diagram of the experimental apparatus is shown in Figure 1. The 80 ps pulses of a 12 W mode-locked Nd:YAG are pulse-compressed and frequency-doubled to 4 ps at 532 nm. This 532 nm beam is actively stabilized, typical average power being 900 mW, and is used to synchronously pump a dye laser. The output of the dye laser, 250 mW at 600 nm with a 350 fs width, is again pulse-compressed to give 120 fs auto correlation pulses. These pulses are amplified in a three-stage amplifier, *Quanta Ray PDA1*, pumped with half of the frequency-doubled output from a Q-switched 10 Hz Nd:YAG. Half of the amplified pulse, 100 μJ peak energy and 150–200 fs duration, is focused into a water cell to produce a continuum of white light, and the remainder is reflected out of the experiment. A component of the continuum is then selected and amplified in a second three-stage amplifier.

In the time-resolved optical Kerr effect experiment, the intense pump or orienting pulse, linearly polarized, creates an ansiotropy in the refractive index of the sample, which may be probed by the weaker, variably delayed, probe laser beam polarized at 45° to the direction of polarization of the intense pump beam. The induced birefringence or change in the refractive index is detected by measuring, by means of a photomultiplier, the intensity of the probe beam passing through crossed polarizes. In our experiments the 10 Hz signal is fed to a boxcar averager and digitized. A computer controls the delay line, with reproducibility of 1 μm, and reads the signal through a standard interface, IEEE 488.

Solutions were made from AnalaR reagents dissolved in spectroscopically pure water, sample weights and volumes being controlled and regulated to volumetric standards. All the solutions

were placed in the same ordinary (commercially available) quartz cuvette, 10 mm path length, for the optical Kerr effect measurements. The sample temperature was not regulated; however, the temperature of the laboratory, and hence the samples, was stable, to within 2°, at 18 °C. Both the pump and the probe laser beams were weakly focused, with standard quartz optics, down to a beam waist of the order of 150 μm into the cell where they overlapped over a distance of the order of 2–3 mm.

The OKE measures the change in the refractive index of the sample due to the nonlinear interaction with the electric field of the incident light beam. The time-resolved optical Kerr effect signal, $S(\tau)$ at a delay time τ, is given by the double integral

$$S(\tau) = \int_{-\infty}^{\infty} I_{\text{probe}}(t-\tau) \sin^2[\int_{-\infty}^{t} R(t-t') I_{\text{pump}}(t')\, dt']\, dt \quad (2)$$

where τ is the delay time between the pump and probe pulses, $R(t)$ is the response function of the system, and I_{probe} and I_{pump} are the intensities of the probe and pump beams, respectively. The second integral in eq 2 represents the phase difference between parallel and perpendicular components of the probe beam, induced by the pump pulse. Assuming that this phase shift is small, we may write

$$S(\tau) = \int_{-\infty}^{\infty} I_{\text{probe}}(t-\tau) [\int_{-\infty}^{t} R(t-t') I_{\text{pump}}(t')\, dt']^2\, dt \quad (3)$$

The time profiles of I_{probe} and I_{pump} are derived from second- and third-order auto correlation traces. These are well fitted, assuming a biexponential shape for the pulses with a fast-rising and slow-decaying profile of the type

$$\exp(\alpha_k t) \quad \text{for } t < 0$$

$$\exp(-\gamma_k \alpha_k t) \quad \text{for } t > 0$$

where $\gamma > 1$ is an asymmetry parameter and $k = 1$ for the pump and $k = 2$ for the probe laser beams. The typical model for the response function, $R_s(t)$, is the sum of exponential, nuclear, or molecular decays plus an instantaneous or electronic response:

$$R_s(t) = R_{\text{electronic}}(t) + R_{\text{molecular}}(t)$$

$$= n_2^e\, \delta(t) + \sum_i \frac{n_2^i}{\tau_i} \exp(-t/\tau_i) \quad (4)$$

where τ_i is the relaxation time of the ith decay component and $\delta(t)$ is the δ function. The other terms are as follows: n_2^e represents the intensity of the instantaneous electronic contribution to the relaxation process, and n_2^i are the intensities of the different slower nuclear or molecular contributions to the observed relaxation, for example, rotational or translational motion.

Our experimental data for the ionic solutions are all compared with that of pure water, the solvent for these experiments. To facilitate direct comparison of the characteristics of the different dynamic behavior of the different solutions, we have normalized all of the nonlinear refractive index components to the electronic or instantaneous part of the relaxation of pure water, that is, to n_2^e(water).

Discussion and Results

Following Buckingham's study of the Kerr effect of solutions,[18] we write the optical Kerr constant for a multicomponent system as

$$K_{\text{Solution}} = \sum_i x_i K^{(i)} + \sum_{ij} x_i x_j K^{(ij)} + \ldots \quad (5)$$

where x_i are the molar fractions of the components with $K^{(i)}$ being the corresponding Kerr constant. In eq 5 the first term on the right represents the additivity rule, while the subsequent terms account for any deviations from additivity.

Over the wide range of solute concentrations investigated, ionic solutions must be considered as systems containing multiple species. We expect a different dynamical behavior at low solute concentration compared to that at high, almost saturated solute concentration. Consider the salt $X^+NO_3^-$, the salt being 100% dissociated; at low concentrations all the X^+ and NO_3^- ions will be completely solvated. This polarization of the aqueous medium by the field of the ions produces large-scale structures in the solution which may well have substantially larger polarizability anisotropies than the bare NO_3^- anion or water molecule. The solvated cation will have, in most cases, no intrinsic polarizability anisotropy, since it is isotropically polarizable. However, as the solution becomes more concentrated, there are simply not enough water molecules available to maintain these extended solvent sheathes. For example, in 6 M $NaNO_3$ solution with each Na^+ ion requiring six water molecules and each NO_3^- ion requiring about two water molecules for solvation, there is barely enough free water present to give a first completed solvent sheath around each ion. The strong dependence of cation hydration and hence anion hydration number upon solute concentration may be seen in the dielectric work of Wei et al.,[19] who observed that for Li^+, in LiCl solution, at a concentration of 1 M the cation hydration number is found to be 7.8 while at a solute concentration of 5 M the hydration number has fallen to 5. We may estimate from the data in ref 19 results for hydration of the Na^+ cation and find a hydration number of 6 at a concentration of 1 M and a hydration number of 4 at 5 M. We have therefore a picture of long-range, polarizable structures established at low concentrations which are disrupted by the strong ionic forces produced by the addition of further solute.

For the time-resolved analysis of our solution results we will rewrite eq 4 as

$$R_s(t) = x_{\text{water}} \left\{ n_2^e(\text{water})\, \delta(t) + \frac{n_2^o(i)}{\tau(i)} \exp -(t/\tau(i)) \right\} +$$
$$x_{\text{solute}} \left\{ n_2^e(\text{solute})\, \delta(t) + \frac{n_2^o(ii)}{\tau(ii)} \exp -(t/\tau(ii)) + \frac{n_2^o(iii)}{\tau(iii)} \exp -(t/\tau(iii)) \right\} \quad (6)$$

where n_2^e(water) and n_2^e(solute) are the instantaneous electronic contributions of the water and of the solute, respectively, to the measured OKE signal. In the second term on the right in eq 6, $n_2^o(i)$ refers to the ith component of the slow, or molecular (nonelectronic), response to the measured OKE signal of water with a time constant $\tau(i)$. The third term on the right in eq 6 represents the electronic or instantaneous response of the solute, the fourth term represents a component of the molecular relaxation of the solute, and the fifth term represents an additional molecular contribution from the solute. That is, there is a purely electronic response and two nuclear contributions $n_2^o(ii)$ and $n_2^o(iii)$ with time constants $\tau(ii)$ and $\tau(iii)$, respectively.

Table 1 and 2 contain the results of our least squares fitting of the experimental data, displayed in Figures 2–5, to eq 6. A recent heterodyne detected OKE experiment[17] has shown for liquid water a rather complex relaxation, with a rotational contribution characterized by a time constant of 1.2 ps, and a faster nonexponential dynamics which decays in the time range of 400 fs, which is attributed to collision-induced and vibrational (Raman) contributions. The signal to noise of our experiments (see Figure 2a) is insufficient to distinguish these two components of the weak delayed signal in pure water. As we are here not specifically interested in the relaxation of pure water, we prefer

TABLE 1: Summary of the Relaxation Dynamics for HCl and NaCl Extracted from the Experimental Data Displayed in Figures 2a,b and 5[a]

solute conc. (mol/L)	n_2^e (units of n_2^e of water)	$n_2^0(i)$ (units of n_2^e of water)	$n_2^0(ii)$ (units of n_2^e of water)	$\tau(ii)$ (ps)
		HCl		
0	1.0	0.25 ± .05		
0.12	1.01 ± .01	0.25 ± .05	0.0 ± .03	
0.6	1.039 ± .031	0.25 ± .05	0.0 ± .03	
1.2	1.108 ± .055	0.25 ± .05	0.111 ± .033	3.5 ± 0.6
1.5	1.128 ± 0.056	0.25 ± .05	0.147 ± .022	3.5 ± 0.2
3	1.206 ± .18	0.25 ± .05	0.205 ± .012	3.6 ± 0.2
6	1.436 ± .273	0.25 ± .05	0.532 ± .043	3.7 ± 0.3
8	1.520 ± .304	0.25 ± .05	0.684 ± .076	3.4 ± 0.5
12	1.701 ± .425	0.25 ± .05	0.936 ± .085	3.5 ± 0.5
		NaCl		
0	1.00	0.25 ± .05		
1.9	1.37 ± .07	0.25 ± .05	0.8 ± 0.4	1.5 ± 0.8
2.85	1.56 ± .08	0.25 ± .05	1.2 ± 0.45	1.5 ± 0.6
5.7	1.93 ± .15	0.25 ± .05	1.8 ± 0.5	1.5 ± 0.6

[a] The raw experimental data are corrected for the signal from pure water, the solvent, and fitted to eq 6. Here, n_2^e is the weight of the purely electronic response; $n_2^0(ii)$ is the weight of the delayed solute contribution, with relaxation time $\tau(ii)$, while $n_2^0(i)$ is the weight of the pure water delayed contribution whose relaxation time is taken to be 700 fs for all solutions. The intensities are given in units of the purely electronic signal of pure water; see text for details.

TABLE 2: Summary of the Relaxation Dynamics for HNO_3 and $NaNO_3$ Extracted from the Experimental Data Displayed in Figures 2a, 3, and 4[a]

solute conc (mol/L)	n_2^e (units of n_2^e of water)	$n_2^0(i)$ (units of n_2^e of water)	$n_2^0(ii)$ (units of n_2^e of water)	$\tau(ii)$ (ps)	$n_2^0(iii)$ (units of n_2^e of water)	$\tau(iii)$ (ps)
			HNO_3			
0	1.0	0.25 ± .05				
0.18	1.025 ± 0.009	0.25 ± .05	0.041 ± .02	2.0 ± 0.5		
0.35	1.044 ± 0.018	0.25 ± .05	0.135 ± .031	2.0 ± 0.3		
0.7	1.052 ± 0.023	0.25 ± .05	0.263 ± .021	2.2 ± 0.1	0.0 ± 0.4	
1.4	1.095 ± 0.044	0.25 ± .05	0.656 ± .065	2.2 ± 0.1	0.0 ± 0.4	
4.7	1.323 ± 0.037	0.25 ± .05	1.323 ± .105	2.0 ± 0.2	1.72 ± 0.39	5.0 ± 0.8
7	1.452 ± 0.04	0.25 ± .05	1.234 ± .101	2.0 ± 0.3	3.12 ± 0.22	6.8 ± 0.5
9.3	1.585 ± 0.091	0.25 ± .05	1.506 ± .126	2.0 ± 0.3	4.99 ± 0.39	8.8 ± 0.3
14	2.029 ± 0.096	0.25 ± .05	1.623 ± .202	4.0 ± 0.4	4.66 ± 0.51	13.4 ± 0.4
			$NaNO_3$			
0	1.00	0.25 ± .05				
0.9	1.104 ± 0.044	0.25 ± .05	0.56 ± 0.033	2.3 ± 0.35	0.0 ± 0.04	
1.8	1.198 ± 0.081	0.25 ± .05	0.30 ± 0.036	2.2 ± 0.25	0.19 ± .07	8.5 ± 1.5
2.9	1.308 ± 0.056	0.25 ± .05	0.85 ± 0.065	2.0 ± 0.15	0.59 ± 0.07	9.5 ± 0.5
4.0	1.402 ± 0.07	0.25 ± .05	1.006 ± 0.07	2.1 ± .2	0.7 ± .08	10 ± 0.5
5.9	1.569 ± 0.062	0.25 ± .05	1.177 ± .141	2.3 ± .3	0.98 ± .09	10 ± 0.3

[a] The raw experimental data are corrected for the signal from pure water, the solvent, and fitted to eq 6. In the case of the aqueous nitrates, two components are fitted to the nuclear part of the ionic relaxation data; that is, there are two delayed contributions from the solute with time constants $\tau(ii)$ and $\tau(iii)$. Again the relaxation time for pure water, $\tau(i)$, is taken to be 700 fs for all solutions investigated. Other symbols have the same meaning as in Table 1.

to model its overall relaxation with a single-exponential decay, with a time constant $\tau(i) = 700 \pm 50$ fs. We wish to make quite clear that this relaxation time has only a heuristic value, not pretending to describe the actual molecular dynamics; however, the inclusion of even a simplified form of the retarded response of pure water is needed to correctly determine the intensity ratio for the other contributions to the OKE signal in the ionic solutions.

In the case of the solutions of sodium chloride and hydrochloric acid, it was found that the data could be well represented by including only one contribution to describe the molecular relaxation, with an associated relaxation time constant to represent the nuclear contribution of the solute ions to the OKE, that is, component (*ii*). However, with the nitrates which can be seen to have produced, by virtue of the intrinsically anisotropic nitrate anion, a much larger OKE, an additional molecular contribution (*iii*), also characterized by an exponential decay, was required to fully represent the data.

(i) Electronic Contribution to the OKE Signal. To probe the two different contributions to the observed optical Kerr signal, the temperature-independent electric field distortion of the molecule, and the temperature-dependent electric field induced orientation of anisotropically polarizable molecules, we have performed two types of experiments. First, we have observed the full temporal evolution of the OKE, as shown in Figures 2–5. We clearly observe the large initial, electronic response of the hyperpolarizability and, at longer time, the decay of the molecular orientational contribution. The time constant and magnitude of this nuclear decay were observed to be a strong function of solute concentration (see Tables 1 and 2).

The other type of experiment was a measure of only the initial instantaneous response. Here, the delay line was set to the zero time position, thereby defining a window with a time width corresponding to the pulse width of the laser, 200 fs. If we assume that it is only the electronic response which may be observed in this time, then we have a direct measure of the solute concentration dependence of the solution hyperpolarizability. Figure 6 represents this data as a function of solute concentration. All the data are normalized to the electronic signal produced by pure water. It is clearly seen, for all four solutions, that the hyperpolarizability scales linearly with solute concentration, within the error bars, increasing as the concentration of cations and anions increases. This demonstrates that in eq 5 only the first term on the right, that representing component additivity,

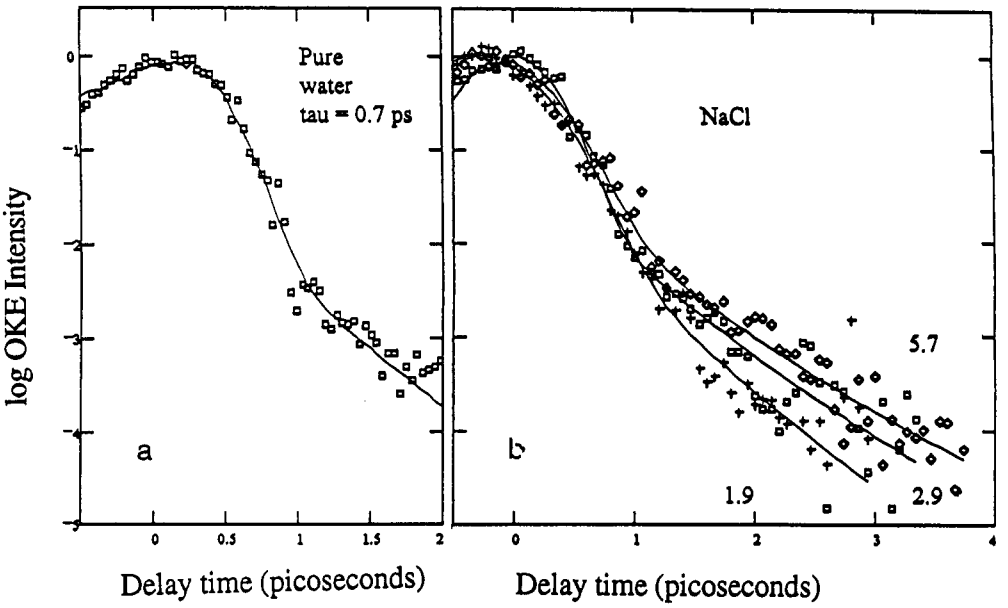

Figure 2. Typical relaxation data from the femtosecond time-resolved optical Kerr effect experiment. One observes the intense electronic response of the system to the applied oscillating electric field and the slow fall of the signal, over many decades, which contains molecular information. In part a we see the signal for pure water, the relaxation of which yields a decay time or relaxation time of 0.7 ps at 18 °C. In part b we see similar data for the femtosecond time-resolved optical Kerr effect experiment on three solutions, of differing strengths (where the concentrations in mol/L are given in the figure) of aqueous sodium chloride. The nuclear or delayed contribution to the observed OKE is seen to increase with increasing solute concentration. Neither the excitation nor the probe laser pulses are δ functions with an infinitely sharp rise time, and consequently, there are some data before the time zero of the arrival of the probe pulse.

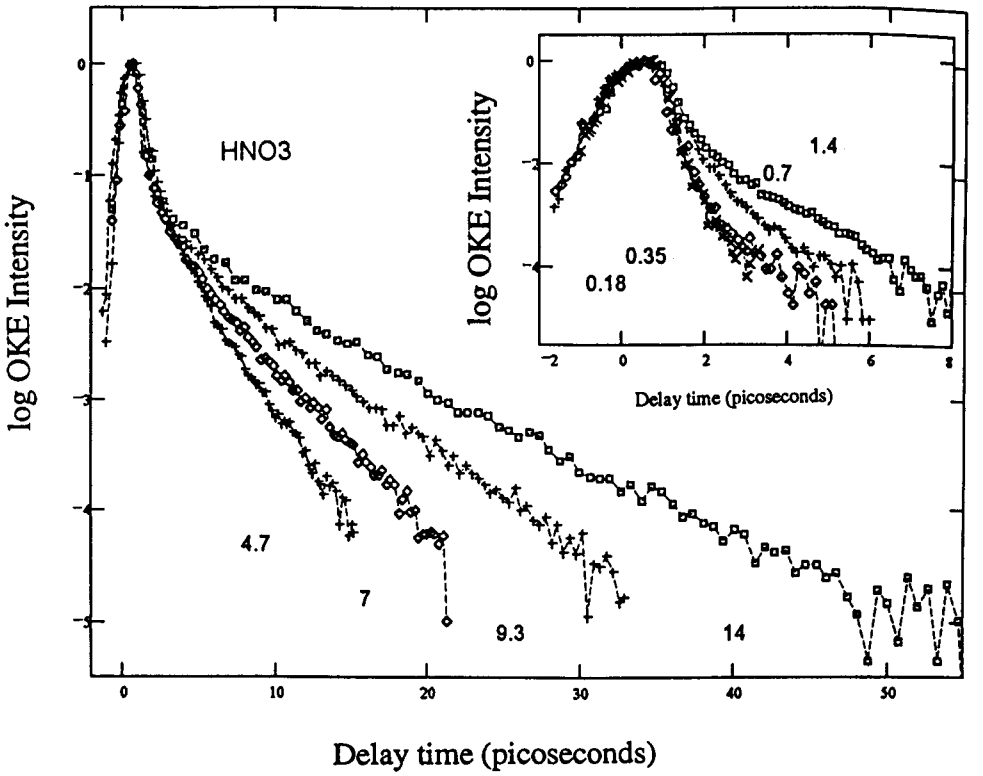

Figure 3. Relaxation data from the femtosecond time-resolved optical Kerr effect experiment on eight solutions, of differing strengths (where the concentrations in mol/L are given in the figure) of nitric acid. The electronic response is normalized to that of water to display the increasing relaxation time with solute concentration. The nuclear or delayed contribution to the observed OKE is seen to increase with increasing solute concentration. Neither the excitation nor the probe laser pulses are δ functions with an infinitely sharp rise time, and consequently, there are some data before the time zero of the arrival of the probe pulse.

is necessary to represent the instantaneous or electronic contribution to the OKE of these aqueous ionic solutions.

Interestingly, the sodium salts give a larger signal compared to the acids, and sodium nitrate a bigger signal than nitric acid. As this measurement is proportional to the mean hyperpolarizability (γ) of the solution, at the various solute concentrations, and assuming that γ scales with electron density, we should be able to relate the magnitude of the observed signal to the mean number of electrons present in the sample. This is indeed the case with the largest signal being given by $Na^+NO_3^-$ solution. The values of $n_2^0(i)$ for the different solutions at zero solute concentration, that is, a measure of the molecular contribution

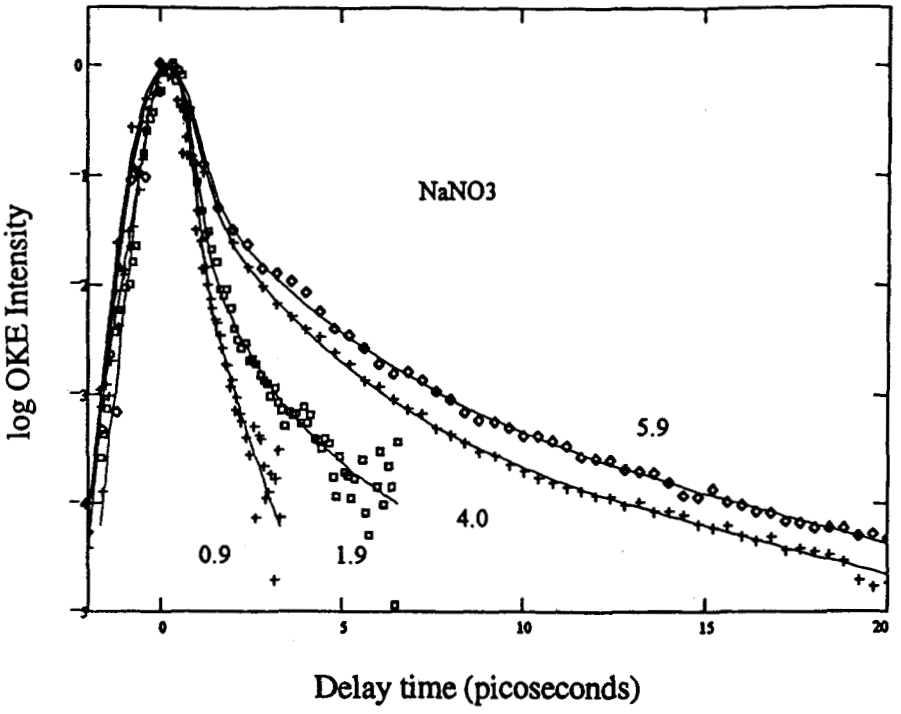

Figure 4. Relaxation data from the femtosecond time-resolved optical Kerr effect experiment on four solutions, of differing strengths (where the concentrations in mol/L are given in the figure) of aqueous sodium nitrate. The electronic response is normalized to that of water to display the increasing relaxation time with solute concentration. The nuclear or delayed contribution to the observed OKE is seen to increase with increasing solute concentration. Neither the excitation nor the probe laser pulses are δ functions with an infinitely sharp rise time, and consequently, there are some data before the time zero of the arrival of the probe pulse.

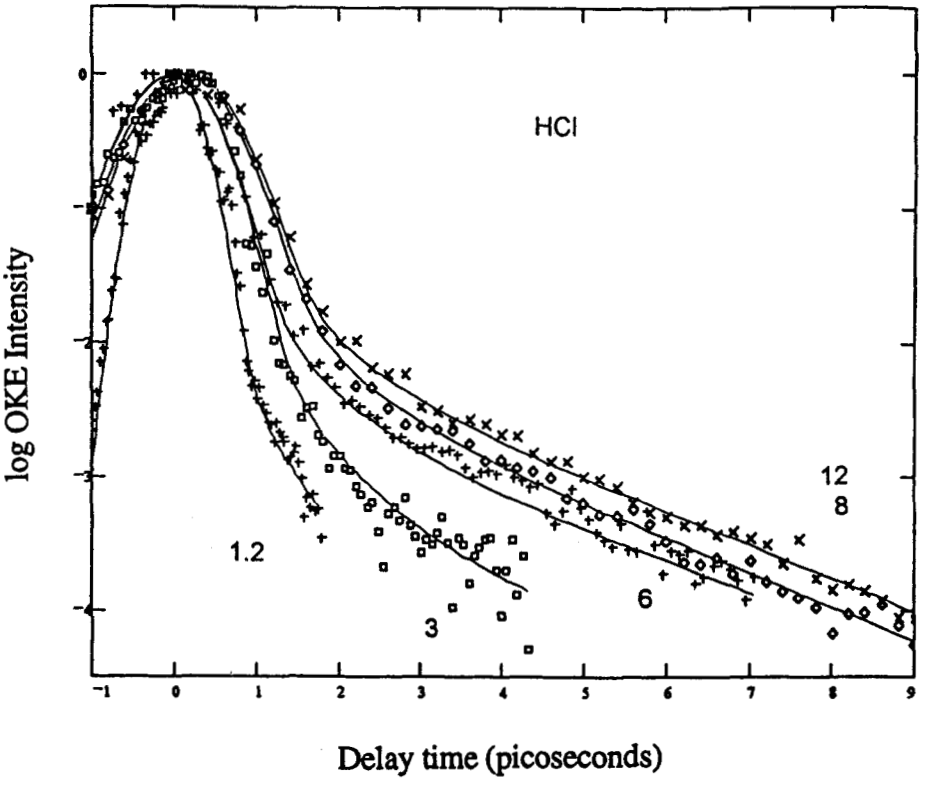

Figure 5. Relaxation data from the femtosecond time-resolved optical Kerr effect experiment on five solutions, of differing strengths (where the concentrations in mol/L are given in the figure) of hydrochloric acid. The electronic response is normalized to that of water to display the increasing relaxation time with solute concentration. The nuclear or delayed contribution to the observed OKE is seen to increase with increasing solute concentration. Neither the excitation nor the probe laser pulses are δ functions with an infinitely sharp rise time, and consequently, there are some data before the time zero of the arrival of the probe pulse.

of the solvent, water, to the observe measurement, were found to be, within experimental error, constant for the four sets of samples investigated. However, the value of $n_2^0(i)$ given in Tables 1 and 2 is the average of those derived independently from the four sets of data.

It should be noted that the true position of the intensity maximum in the instantaneous OKE signal is a function of solute concentration because of the contribution of the delayed, molecular, component of the signal. For example, in nitric acid the variation in the position of the intensity maximum between

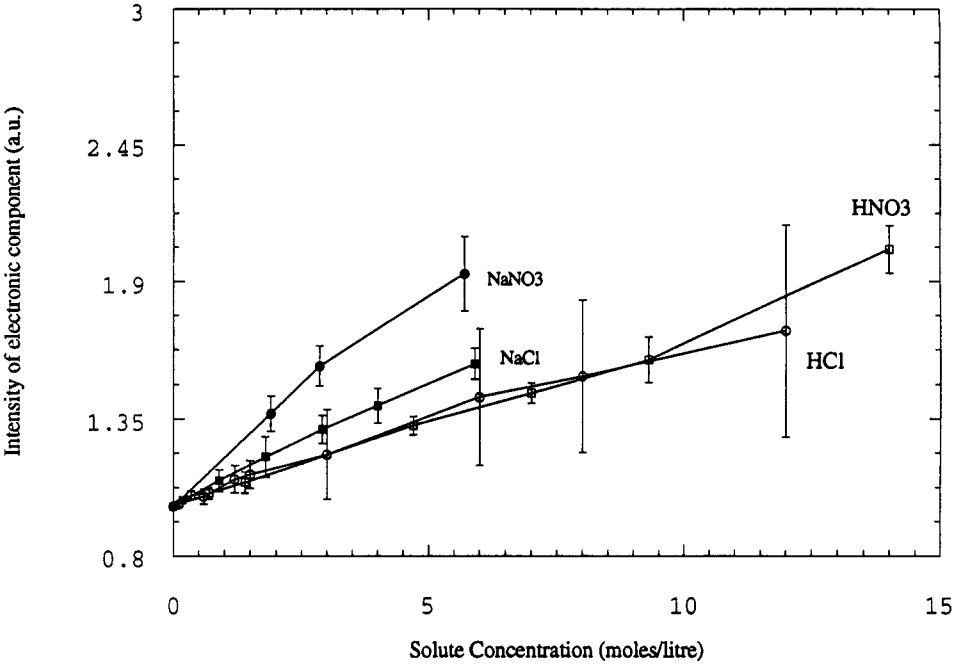

Figure 6. Solute concentration dependence of the maximum intensity of the electronic contribution to the observed optical Kerr effect; all values are scaled to that of pure water.

a solution of 14 M and pure water is 70 fs. Consequently, the effect of using the same time delay for the measurements on all solutions is less than 2% and may be neglected.

The well-behaved dependence of the electronic contribution to the OKE signal on solute concentration in aqueous solutions is reminiscent of the concentration behavior of the Cotton–Mouton effect on the same aqueous ionic solutions.[20]

(ii) Nuclear Contributions to the OKE of Sodium Nitrate and Nitric Acid Solutions. Figures 2a, 3, and 4 clearly show that the delayed OKE of $NaNO_3$ and HNO_3 is, at all measured concentrations, much larger than the signal from pure water. For these solutions the anisotropic NO_3^- ion will contribute strongly to the measurements at all solute concentrations, the cations being spherically symmetric and possessing an isotropic polarizability. Consequently, it is the dynamics of the nitrate ion which is the dominant contribution to the OKE of these solutions. Table 2 gives the results of our least squares fitting for these data. The experimental data have been fit to a three-component model: in addition to the purely electronic component there is a component (*ii*) with relaxation time constant $\tau(ii)$ and a longer time relaxational component (*iii*) with time constant $\tau(iii)$. It is seen in Table 2 that $\tau(ii)$ is almost independent of solute concentration for both solutions while $\tau(iii)$ is strongly dependent on solute concentration in both samples. Indeed, whereas the longer time constant, $\tau(iii)$, increases continually with increasing HNO_3 concentration, the same relaxation time constant saturates in $NaNO_3$ solution at a sodium nitrate concentration of the order of 3 mol/L.

We have interpreted these nitrate results as follows: besides the purely electronic response and the fast relaxation component arising from the pure solvent, there is an intermediate concentration-independent relaxation, $\tau(ii) \sim 2.2$ ps, corresponding to the rotational relaxation of the NO_3^- anions, and a slow decay, whose time constant $\tau(iii)$ increases with solute concentration. A similar behavior has been observed by time-resolved OKE measurements in molten $2[Ca(NO_3)_2]\cdot 3[KNO_3]$[21] a well-known glass-forming system. It should be noticed that our value of $\tau(ii)$ is slightly higher than that obtained from Raman experiments.[22]

In Figure 7 the behavior of the two decay times corresponding to the above relaxation mechanisms, $\tau(ii)$ and $\tau(iii)$, in HNO_3 are plotted against solute concentration, and in Figure 8a we display the concentration behavior of the relative weights of the two components in HNO_3. The increase of $\tau(iii)$ with concentration for nitric acid is clear evidence of the cooperative nature of the associated process. It is seen that the appearance of $\tau(iii)$ coincides with the disappearance of "free" water molecules (represented by the dashed line in Figure 8a), that is, when additional solute cannot obtain a full solvation sheath due to the lack of free unassociated bulk water molecules. For concentrations above 5 M the NO_3^- anions see each other directly as opposed to sensing each other within a solvent sheath, thereby setting up correlated multi-ionic structures. In this sense one may speak of the glassy or highly disordered nature of these concentrated aqueous solutions which become very viscous at these high levels of solute concentrations.

In our solutions of sodium nitrate, the concentration dependence behavior of the nitrate anion dynamics mimics that of nitric acid (see Figures 7 and 8b), the difference between these two nitrates being that in the case of the salt: the $\tau(iii)$ relaxation time saturates at a relatively low solution concentration. However, we note that at these solute levels in aqueous $NaNO_3$ solution we are not far from saturation, whereas in nitric acid we are still a little way from saturation even at 14 M. Similarly, in these concentrated solutions where the ions will not possess complete solvation structures, that is, in this glasslike state, the sodium cations and the nitrate anions will have become "frozen in" to a disordered system. That is, their mobility will have become somewhat reduced; the solutions are seen to be very viscous, and their relaxation will become arrested as the free water molecules become involved in the strongly bound interionic matrix. The protons, however, will, by virtue of their mass, be more labile in these viscous glassy solutions and will continue to move rapidly through the solution, distorting the medium as they move, giving a measurable OKE, which increases with solute concentration, over the range investigated in our experiments.

(iii) Nuclear Contributions to the OKE of Sodium Chloride and Hydrochloric Acid Solutions. For those salts which have no intrinsically anisotropically polarizable ions, the measured OKE arises through molecular interactions, e.g. NaCl and HCl. These ion pairs at infinite separation have no anisotropy in their polarizability, and we will therefore be unable to directly probe the dynamics of these ions. They will, however, still have a Kerr effect, optical and static, due to the purely electronic or hyperpolarizability term which is temperature independent in

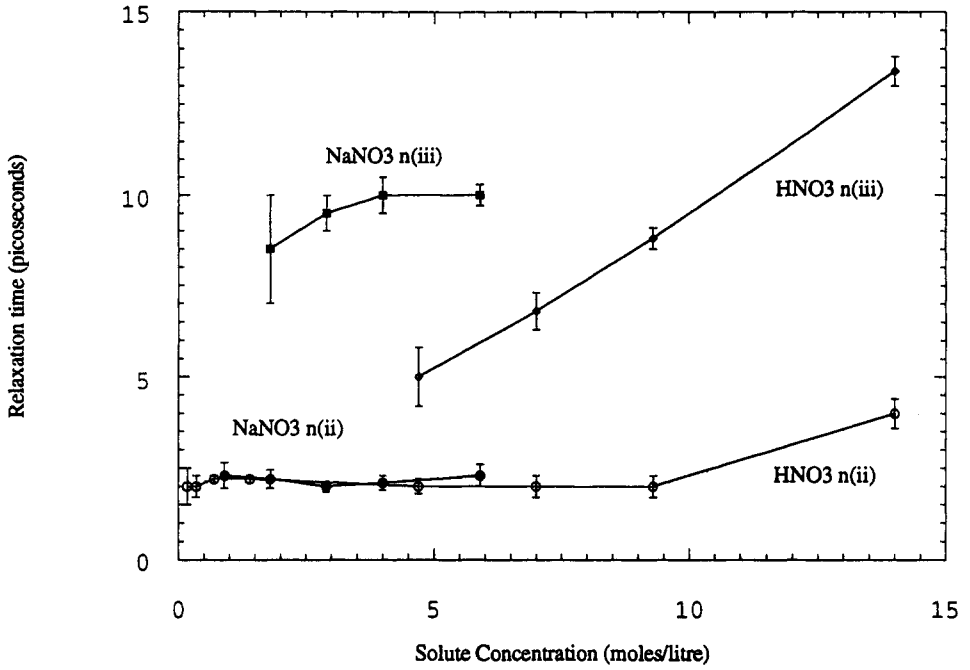

Figure 7. Solute concentration dependence of the derived relaxation times for solutions of nitric acid and sodium nitrate. For both sets of solutions, $\tau(ii)$ is seen to be essentially independent of concentration except at the highest, glasslike, concentrations and $\tau(iii)$ increases with solute concentration.

purely noninteracting particles[1,2] (see the data in Figure 6). For the nitrate solutions, however, the anisotropic NO_3^- ion will contribute strongly to the measurements at all solute concentrations. All the solvated ions studied will have a hyperpolarizability contribution to the measured OKE.[2,5] Indeed, this hyperpolarizability, for a completely solvated ion, may be quite appreciable. We may also interpret this difference in the OKE of pure water and in aqueous solutions of NaCl and HCl as arising because of the breakup of the complex hydrogen-bonded structure of water. The statistical average over the angular coordinates of the molecules in the presence of the applied electromagnetic fields which are involved in deriving expressions for the Kerr effect signal in pure fluids are made more complicated in water because of the presence of the strong hydrogen bonds which make up the liquid producing an ordered structure.[2,5] However, when small spherical ions are present, they polarize the medium and disrupt these hydrogen bonds, obtaining a solvent sheath in the process. If we assume that the ions make no net contribution to the measurement, i.e. they are unobservable electro-optically, being isotropically polarizable, then the OKE for aqueous solutions of spherical ions such as $Na^+_{(aq)}Cl^-_{(aq)}$ and $H^+_{(aq)}Cl^-_{(aq)}$ give a measure of the OKE for disordered water.

The time evolution of the OKE signal measured in NaCl solutions is well reproduced, assuming an exponential relaxation with a time constant of about 1.5 ps. The measured signal to noise precludes the determination of a more precise value for this time constant, and the value of 1.5 ps given in Table 1 represents an average value for the three solute curves displayed in Figure 2b. It is natural to compare this relaxation time with that measured by Chang and Castner[17] in pure water (1.2 ps) which they attributed to the rotational dynamics of water molecules. The same idea could be applied to our data for NaCl solutions, assuming that the increased electric susceptibility of the solutions allow the observation of the rotational relaxation of the water molecules. The increase, with solute concentration, of the intensity of the retarded contribution to the signal is evident in Figure 2b. On the other hand, the increase of the rotational time on going from pure water to NaCl solution can be attributed to changes in the friction coefficients due to the presence of charged species.

However, we cannot exclude that the atomic ions themselves give a more direct contribution to the retarded OKE signal. It was previously noted that the Cotton–Mouton constant for solvated NaCl is positive while that for KCl is smaller and negative;[20] however, a difference in the solvation dynamics of Na^+ and K^+ is well-known.[23,24] The smaller, polarizing Na^+ cation is termed a structure-making cation while the K^+ cation, being larger and less able to polarize the medium, is considered a structure-breaking cation.[23,24]

At the ionic concentrations used in the Cotton–Mouton measurements, which are similar to the concentrations used in these measurements, the dielectric measurements of Wei et al.[19] give hydration numbers for these cations of 4.75 ± 0.25 for $Na^+_{(aq)}$. Similarly, the neutron scattering measurements of Neilson and Enderby[25] and Skipper and Neilson[23] give hydration numbers of 5 for $Na^+_{(aq)}$ and 4 for $K^+_{(aq)}$ at these solute concentrations. With four water molecules, which from space requirements would be tetrahedrally disposed around the K^+ cation, this solvated aquation will have no anisotropic polarizability, being spherically symmetric. In the case of Na^+, however, solvated with five water molecules, the structure will be such as to possess an anisotropic polarizability.

Provided we are not at solution concentrations which are so large as to prevent the formation of complete solvent sheaths, it is not unreasonable, considering the nonspherical symmetry of the solvated sodium cation, that there exists a measurable OKE for aqueous NaCl. The Cl^- anion at these concentrations is believed to be solvated with six water molecules[25] and, consequently, with such an octahedral disposition of water ligands will have no polarizability anisotropy, remaining isotropically polarizable. These solvent sheaths of four, five, or six water molecules will of course be time dependent; that is, at thermal temperatures water molecules will be breaking way from the immediate solvent sheath and other water molecules will be complexing to the ions. Consequently, it would be perhaps better to say that solvated sodium cations will have an anisotropic polarizability which will fluctuate, but on average will be finite, whereas solvated potassium and chloride ions will have polarizability anisotropies which will fluctuate; however, the fluctuations will be much smaller than in the case of $Na_{(aq)}$.

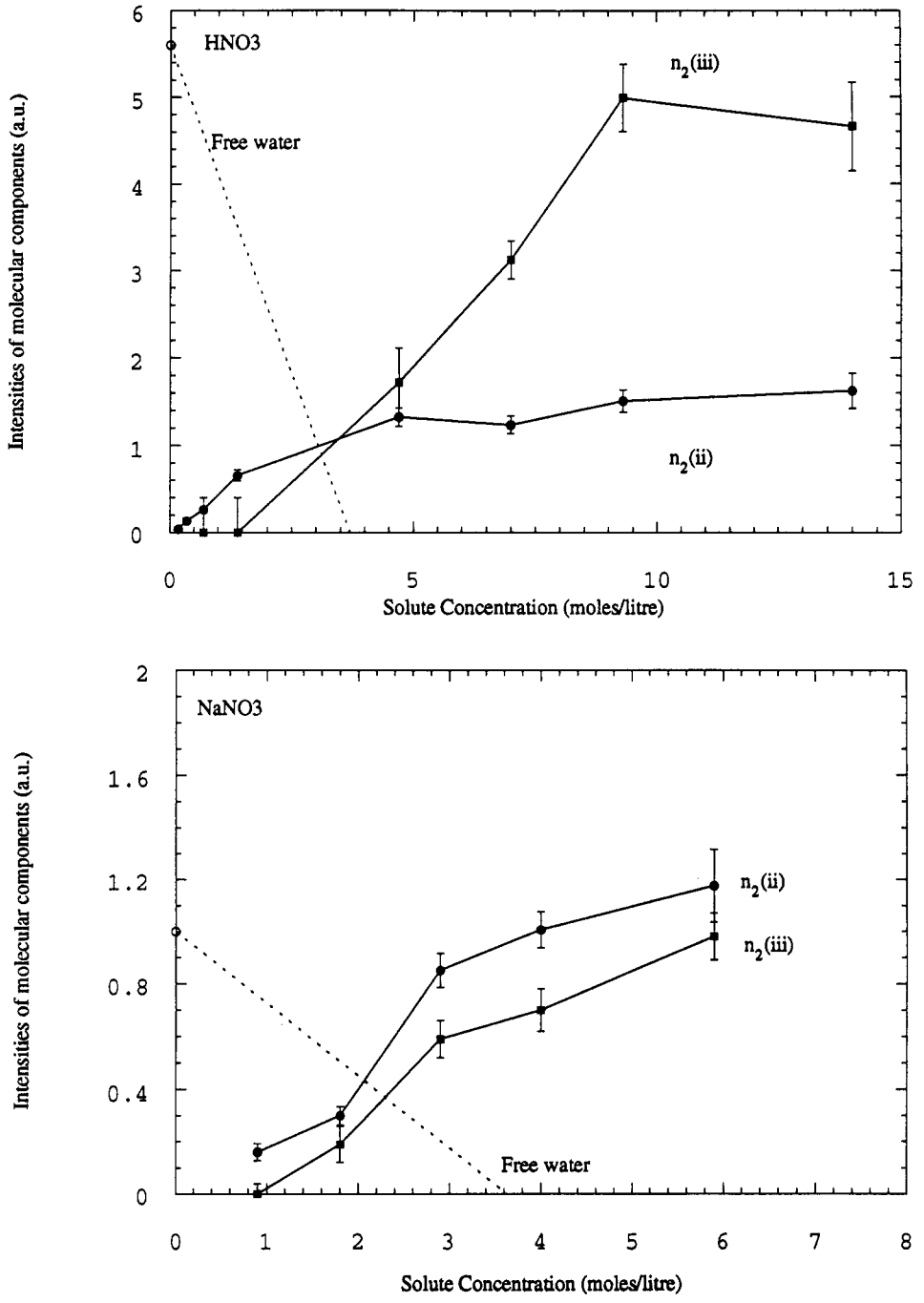

Figure 8. (a, Top) Effect of the availability of free water (dashed line) on solute concentration dependence of the weights of the two terms contributing to the relaxation mechanism for nitric acid solutions. The appearance of $n(iii)$ is seen to coincide with the loss of free water molecules. See text for details. (b, Bottom) Effect of the availability of free water (dashed line) on solute concentration dependence of the weights of the two terms contributing to the relaxation mechanism for sodium nitrate. See text for details.

The observations are similar for solutions of HCl: at the very lowest concentrations the solution of HCl behaves like water but as the solute concentration increases the magnitude of the OKE increases and the relaxation dynamics become very different (see Figures 2a and 5). We also see, from Table 1, that the relaxation times for the solute extracted from the displayed data are different for these two aqueous chlorides; in NaCl, the solute relaxes with a time constant of 1.5 ± 0.7 ps while, in HCl, at similar levels of solute concentration, the relaxation is longer, 3.6 ± 0.4 ps.

A difference in the dynamics of these two solutions is not unexpected. Although the anion is common, and at similar concentration levels the solvated chloride ion should make similar contributions to both samples, the proton will behave very differently from the sodium cation. Due to the extreme polarizing nature of the proton and its mobility, it will, compared to the heavier less polarizing sodium cation, move readily through the glasslike medium at high concentrations, distorting the medium as it moves.

Due to the much lower signal to noise of the OKE experiments on the chlorides compared to the nitrates, a detailed analysis of the solute concentration dependence of the different molecular relaxation modes is not possible.

This analysis of the electro-optic properties of aqueous solutions which has been made is very qualitative and makes many approximations. However, it illustrates the type of information which is available from these experiments and points the way for further work.

References and Notes

(1) Buckingham, A. D. *Proc. Phys. Soc.* **1955**, *A68*, 910.

(2) Buckingham, A. D. In *Molecular Electro-optics*; O'Konski, C. T., Ed.; Marcel Dekker: New York, 1976; p 27.
(3) Fleming, G. R. *Chemical Applications of Ultrafast Spectroscopy*; Oxford University Press: Oxford, U.K., 1986.
(4) Chen, Y-J.; Orttung, W. H. *J. Phys. Chem.* **1972**, *76*, 216. Khanna, R. K.; Dempsey, E.; Parry Jones, G. *Chem. Phys. Lett.* **1978**, *53*, 542.
(5) Buckingham, A. D. *Proc. Phys. Soc.* **1956**, *B69*, 344.
(6) Aroney, M. J.; Battaglia, M. R.; Ferfoglia, R.; Miller, D.; Pierens, R. K. *Trans. Faraday Soc.* **1976**, *72*, 724.
(7) Paillette, M. *Ann. Phys. (Paris)* **1969**, *4*, 671.
(8) Pailette, M. *J. Chim. Phys. (Paris)* **1968**, *65*, 1629.
(9) Kenney-Wallace, G. A.; Paone, S.; Kalpouzos, C. *Discuss. Faraday Soc.* **1988**, *85*, 185.
(10) Back, R.; Kenney-Wallace, G. A.; Lotshaw, W. T.; McMorrow, D. *Chem. Phys. Lett.* **1992**, *191*, 423.
(11) Kalpouzos, C.; McMorrow, D.; Lotshaw, W. T.; Kenney-Wallace, G. A. *Chem. Phys. Lett.* **1988**, *150*, 138.
(12) Kalpouzos, C.; McMorrow, D.; Lotshaw, W. T.; Kenney-Wallace, G. A. *Chem. Phys. Lett.* **1989**, *155*, 240.
(13) Ruhman, S.; Joly, A. G.; Nelson, K. A. *J. Chem. Phys.* **1987**, *86*, 6563.
(14) McMorrow, D. M.; Lotshaw, W. T. *Chem. Phys. Lett.* **1990**, *174*, 85.
(15) McMorrow, D. M. *Opt. Commun.* **1991**, *86*, 236.
(16) Chen, Y. J.; Castner, E. W., Jr. *CLEO'93 Technical Digest* QPD12 – 1/25.
(17) Chang, Y. J.; Castner, E. W. *J. Chem. Phys.* **1993**, *99*, 113.
(18) Buckingham, A. D. *Trans. Faraday Soc.* **1956**, *52*, 611.
(19) Wei, Y-Z.; Chiang, P.; Sridhar, S. *J. Chem. Phys.* **1992**, *96*, 4569.
(20) Williams, J. H.; Torbet, J. *J. Phys. Chem.* **1992**, *96*, 10477.
(21) Ricci, M.; Foggi, P.; Righini, R.; Torre, R. *J. Chem. Phys.* **1993**, *98*, 4892.
(22) Adachi, A.; Kiyoyama, H.; Nakahara, M.; Masuda, Y.; Yamatera, H.; Shimizy, A.; Taniguchi, Y. *J. Chem. Phys.* **1989**, *90*, 392.
(23) Skipper, N. T.; Neilson, G. W. *J. Phys.: Condens. Matter 1* **1989**, 4141.
(24) Howell, I.; Neilson, G. W.; Chieux, P. *J. Mol. Struct.* **1991**, *250*, 281.
(25) Neilson, G. W.; Enderby, J. E. *Adv. Inorg. Chem.* **1989**, *34*, 195.